

MEASUREMENT AND MODELLING OF THE RESPONSE OF THE CAT EARDRUM TO LARGE STATIC PRESSURES

Hanif M. Ladak^{1,2}, W. Robert J. Funnell³, Willem F. Decraemer⁴ and Joris J. J. Dirckx⁴

¹Depts. of Medical Biophysics and Electrical & Computer Engineering, The University of Western Ontario, London, Ontario, Canada, N6A 5C1 hladak@uwo.ca

²Imaging Research Labs, Robarts Research Institute, London, Ontario, Canada, N6A 5K8

³Depts. of BioMedical Engineering and Otolaryngology, McGill University, Montréal, Québec, Canada, H3A 2B4

⁴Laboratory of BioMedical Physics, University of Antwerp, Antwerp, Belgium B-2020

1. INTRODUCTION

In tympanometry, a clinically important test of middle-ear function, static pressures are used which are so high that the responses become nonlinear. In current finite-element (FE) models of the middle ear, however, the relationship between applied pressure and the resulting displacements is assumed to be linear. Measurement and modelling of the response to high pressures will lead to a better understanding of the mechanics of tympanometry.

We have measured the shape and displacement patterns of the cat eardrum using phase-shift shadow-moiré topography, a non-contacting optical technique (Ladak *et al.*, 2004). The experiments involved cyclically pressurizing the middle ear up to ± 2.2 kPa after immobilizing the malleus. The immobile-malleus condition allows investigation of eardrum response in isolation from any possible nonlinearities of the cochlea and middle ear. The data indicate that the eardrum response is nonlinear at these pressures and that eardrum displacements are larger than its thickness. This suggests that, as a minimum, geometric nonlinearity must be included in FE models of the eardrum. The role of material nonlinearity is not clear from the data.

The objective of this work is to determine whether geometric nonlinearity alone can account for the observations, by incorporating it into subject-specific FE eardrum models and comparing simulation results to measurements.

2. FINITE-ELEMENT MODELS

2.1. Mesh geometry

Individualized FE meshes were constructed from unpressurized shape data using the procedure described by Funnell and Decraemer (1996). Here we present results for one cat. A sample image of the shape of the cat eardrum is shown in Figure 1. The grey levels in the image vary from black (points farthest from reader) to white (points closest to reader). A vertical profile through the pars tensa, just inferior to the umbo, is shown in black to the left of the image, and a horizontal profile through the posterior pars

tensa is shown below the image. The profiles are taken through the locations indicated by the dashed lines. Also shown is a lateral view of an FE mesh constructed from the data along with profiles (grey) through the mesh; the mesh profiles are offset so as not to overlap with the image profiles. Each triangle in the mesh represents an S3R shell element of the ABAQUS FE software package (Hibbit, Karlsson & Sorensen Inc., Pawtucket, RI, U.S.A.). No elements are generated for the manubrium as it is assumed to be completely immobile.

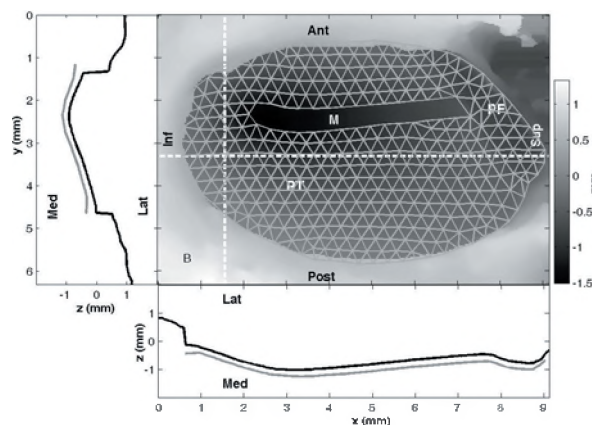


Figure 1 Shape image of a cat eardrum with FE mesh superimposed. Anterior (Ant), posterior (Post), superior (Sup), inferior (Inf), medial (Med) and lateral (Lat) directions are approximate.

2.2. Mechanical properties

The eardrum is modelled as being isotropic, homogeneous throughout its thickness, and uniform across its surface. It is also assumed to be linearly elastic. The pars tensa has a Young's modulus of 20 MPa, a thickness of 40 μm and a Poisson's ratio of 0.3; the pars flaccida has a Young's modulus of 1 MPa, a thickness of 80 μm and a Poisson's ratio of 0.3 (Funnell and Decraemer, 1996). The periphery of the eardrum is assumed to be fully clamped.

2.3. Solution procedure

Displacements were computed for uniform static middle-ear pressures from 0 to +2.2 kPa in steps of +0.1 kPa

and from 0 to -2.2 kPa in steps of -0.1 kPa. A combined incremental/iterative solution procedure was used to compute the response at each step.

3. RESULTS

3.1. Displacement patterns

Figure 2 shows simulated and measured iso-amplitude displacement patterns for a pressure of $+2.2$ kPa. The simulated patterns exhibit a local maximum of $255 \mu\text{m}$ in the supero-posterior pars tensa. The measured maximum, however, is smaller ($140 \mu\text{m}$) and occurs more inferiorly than it does in the simulations.

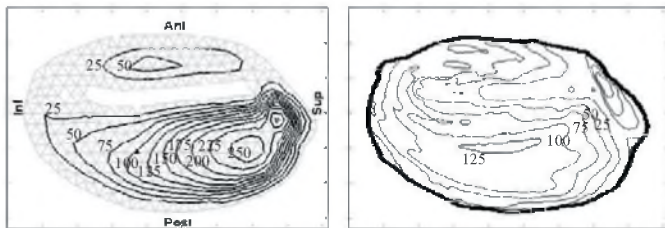


Figure 2 (a) Simulated and (b) measured iso-amplitude displacement contours for $+2.2$ kPa. Displacements are in μm .

For small negative pressures (e.g., -0.1 and -0.2 kPa), simulated and measured displacements patterns are similar to those for positive pressures. For larger negative pressures, the location of the maximum is shifted inferiorly compared to that for positive pressures, for both simulated and measured displacements.

3.2. Pressure-displacement curves

Figure 3 shows pressure-displacement curves for the point indicated by the triangle in Figure 2(a). Three cycles of measured data are shown in grey, and the simulated curve is shown in black. The measured curves vary from one cycle of pressurization to the next and exhibit hysteresis, with displacements being larger during unloading than during loading. There is only one simulated curve because the material is assumed to be elastic, with no hysteresis. Both simulated and measured curves exhibit nonlinearity, with displacements growing less than in proportion to the applied pressure.

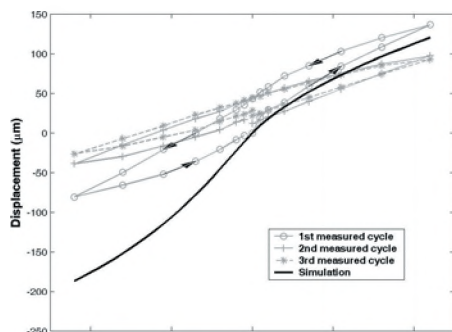


Figure 3 Simulated and measured pressure-displacement curves.

For positive pressures, the simulated pressure-displacement curve agrees reasonably well with the measured data. For negative pressures, the calculated displacements are larger in magnitude than the measured ones.

3.3. Effect of non-uniformity

The location of the maximum pars-tensa displacement in the simulated patterns can be shifted inferiorly by including non-uniformities in either the Young's modulus or the thickness. For example, Figure 4 shows the effect on the displacement patterns computed for $+2.2$ kPa after increasing the thickness of the superior third of the posterior pars tensa from $40 \mu\text{m}$ to $80 \mu\text{m}$.

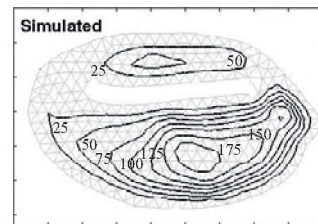


Figure 4 Simulated iso-amplitude displacement contours after including non-uniformity. Displacements are in μm .

4. DISCUSSION

The inclusion of geometric nonlinearity in an FE model allows simulation of the stiffening behaviour of the eardrum with increasing pressure.

The pars-tensa maximum in the simulated displacement patterns for positive pressures is located superior to the measured location. Increasing the stiffness or the thickness of the superior third of the posterior pars tensa in the model has the effect of shifting the maximum inferiorly and of decreasing its magnitude, improving the match with the experimental data. Such a thickness increase is consistent with recent experimental thickness measurements (Kuypers *et al.*, 2005).

REFERENCES

- Funnell, W.R.J., and Decraemer, W.F. (1996). "On the incorporation of moiré shape measurements in finite-element models of the cat eardrum," *J. Acoust. Soc. Am.* **100**, 925–932.
- Kuypers LC, Decraemer WF, Dirckx JJJ & Timmermans J-P (2005). "Thickness distribution of fresh eardrums of cat obtained with confocal microscopy," *JARO* **6**, in press.
- Ladak, H.M., Decraemer, W.F., Dirckx, J.J.J., and Funnell, W.R.J. (2004). "Response of the cat eardrum to static pressures: Mobile versus immobile malleus," *J. Acoust. Soc. Am.* **116**, 3008–3021.

ACKNOWLEDGEMENTS

Funding for this work was provided by the Canadian Institutes of Health Research (WRJF), the Natural Sciences and Engineering Research Council of Canada (HML) and the Québec-Belgium Exchange Programme (HML).